Chimeric Mouse With Humanized Liver Is an Appropriate Animal Model to Investigate Mode of Action for Porphyria-Mediated Hepatocytotoxicity

Ayumi Eguchi[1] ⬤, Satoki Fukunaga[1], Keiko Ogata[1], Masahiko Kushida[1], Hiroyuki Asano[1], Samuel M. Cohen[2] ⬤, and Tokuo Sukata[1]

Abstract

Porphyrinogenic compounds are known to induce porphyria-mediated hepatocellular injury and subsequent regenerative proliferation in rodents, ultimately leading to hepatocellular tumor induction. However, an appropriate in vivo experimental model to evaluate an effect of porphyrinogenic compounds on human liver has not been fully established. Recently, the chimeric mouse with humanized liver (PXB mice) became widely used as a humanized model in which human hepatocytes are transplanted. In the present study, we examined the utility of PXB mice as an in vivo experimental model to evaluate the key events of the porphyria-mediated cytotoxicity mode of action (MOA) in humans. The treatment of PXB mice with 5-aminolevulinic acid, a representative porphyrinogenic compound, for 28 days caused protoporphyrin IX accumulation, followed by hepatocyte necrosis, increased mitosis, and an increase in replicative DNA synthesis in human hepatocytes, indicative of cellular injury and regenerative proliferation, similar to findings in patients with porphyria or experimental porphyria models and corresponding to the key events of the MOA for porphyria-mediated hepatocellular carcinogenesis. We conclude that the PXB mouse is a useful model to evaluate the key events of the porphyria-mediated cytotoxicity MOA in humans and suggest the utility of PXB mice for clarifying the human relevancy of findings in mice.

Keywords

chimeric mouse with humanized liver, chemical-induced porphyria, porphyria-mediated cytotoxicity MOA

Introduction

A number of chemicals, drugs, and pesticides are known to interfere with hepatic heme biosynthesis in rodents, mainly by inhibiting particular enzymes of the heme biosynthesis pathway, which leads to accumulation of intermediate porphyrinogens and their oxidized product porphyrins in many tissues including the liver (chemically induced porphyria). The accumulation of porphyrins (mainly protoporphyrin IX [PPIX]) in hepatocytes results in sustained hepatocellular injury (cytotoxicity) by inducing oxidative stress[1] and/or protein oxidation and aggregation[2-4] followed by regenerative cell proliferation, leading to an aberrant healing process and ultimately the development of liver tumors.[5,6] Therefore, the mode of action (MOA) for porphyrinogenic compound-induced liver tumors commonly follows a cytotoxic MOA (porphyria-mediated cytotoxicity MOA), indicating that the key events which precede tumor development are: (1) accumulation of porphyrins, (2) followed by hepatocellular injury, with (3) subsequent regenerative cell proliferation.[5-8]

In humans, it has been reported that dominant or recessive genetic variants of the enzymes of the heme biosynthesis pathway cause dysfunction of the enzyme(s), resulting in porphyria of varying severity.[7] In general, patients with porphyria have chronic liver abnormalities including hepatocellular toxicity, cell death with regenerative hepatocellular proliferation, resulting in increased risk for development of hepatocellular carcinoma.[9] These key events for the porphyria-mediated cytotoxicity MOA in rodents are considered to have some similarities with human porphyria leading to liver tumorigenesis, and therefore this carcinogenicity MOA is considered qualitatively plausible in humans.[6] In the case of a carcinogenicity MOA in rodents which is qualitatively relevant to humans, a more

[1] Environmental Health Science Laboratory, Sumitomo Chemical Co, Ltd, Osaka, Japan
[2] Department of Pathology and Microbiology, Havlik-Wall Professor of Oncology, University of Nebraska Medical Center, Omaha, NE, USA

Corresponding Author:
Ayumi Eguchi, Environmental Health Science Laboratory, Sumitomo Chemical Co, Ltd, Osaka, 554-8558, Japan.
Email: eguchia@sc.sumitomo-chem.co.jp

quantitative assessment is required for purposes of human relevance analysis in accordance with the International Programme on Chemical Safety Human Relevance Framework.[10] Therefore, establishment of an appropriate in vivo experimental model is important to evaluate the effect of porphyrinogenic compounds on these key events in human liver, which enables a more accurate quantitative assessment and human relevance analysis.

Recently, the chimeric mouse with humanized liver model (product name: PXB mouse, hereafter referred as PXB mouse) has been developed by PhoenixBio Co, Ltd (https://phoenixbio.co.jp) and became commercially available as the humanized mouse model. The PXB mouse is produced by transplanting human hepatocytes into the albumin (Alb) enhancer/promoter-urokinase-type plasminogen activator complementary DNA (cDNA) transgenic/SCID mouse with immunodeficiency and liver disorders,[11-13] whose liver is repopulated by human hepatocytes at a ratio of more than 70%. The transplanted human hepatocytes express a variety of human messenger RNA (mRNA) and proteins, in a similar manner to those of the normal human liver.[11-13] Chimeric mouse livers consist of human hepatocytes with a small percentage of mouse hepatocytes and mouse hepatic sinusoidal cells (mainly Kupffer cells, endothelial cells, and stellate cells), and the human hepatocytes have been shown to cooperate with mouse hepatic sinusoidal cells in carrying out liver functions.[12] Given these characteristics, PXB mice have been widely used for evaluation of hepatotoxicity induced by chemical compounds[14-17] or therapeutic antibodies,[18] and also for MOA studies for hepatocellular carcinogenesis.[19-21] However, the key events of the porphyria-mediated cytotoxicity MOA have not yet been evaluated using PXB mice, and thus the present study was conducted to assess whether these key events could be detected in PXB mice by using a representative porphyrinogenic compound. As mentioned above, many porphyrinogenic compounds inhibit particular enzymes of the heme biosynthesis pathway, but species differences in enzyme inhibition are well-known, suggesting that humans are generally less sensitive than rodents.[7] Hence, we focused on the chemical compound which nonenzymatically causes porphyrin accumulation when selecting a representative porphyrinogenic compound to induce porphyria-mediated cytotoxicity in humans.

5-Aminolevulinic acid (ALA) is an endogenous nonproteinogenic amino acid which is the first compound in the heme biosynthesis pathway. In mammalian liver, ALA is synthesized by combining glycine with succinyl-CoA and synthesis is catalyzed by $5'$-aminolevulinate synthase 1 (ALAS1), the rate-limiting enzyme in the heme biosynthesis pathway.[22] It is known that administration of ALA to mammals can bypass the rate-limiting step, inducing perturbation of porphyrin biosynthesis characterized by accumulation of intermediates after ALA (mainly PPIX) in this pathway. It has also been demonstrated that administration of ALA to rats causes porphyrin accumulation in the liver followed by cytotoxicity.[23,24] Taking advantage of these characteristics, ALA is utilized for photodynamic diagnosis-assisted surgery as an aid for the visualization of malignant tissue during tumor resection, which is approved by the Japanese Pharmaceuticals and Medical Devices Agency,[25] the US Food and Drug Administration,[26] and the European Medicines Agency.[27] In clinical trials or clinical application, one side effect of ALA is hepatocellular toxicity, which is indicated by increases in liver serum enzymes such as alanine aminotransferase (ALT) and aspartate aminotransferase (AST).[28-33] We hypothesized, based on these data and observations, that ALA would be an adequate porphyrinogenic compound to induce porphyria-mediated cytotoxicity in human hepatocytes transplanted in PXB mouse liver.

In the present study, we investigated the effects of ALA on the key events of porphyria-mediated cytotoxicity MOA when administered via diet to PXB mice for 28 consecutive days, by examining PPIX accumulation in the liver, blood biochemistry, liver histopathology, and replicative DNA synthesis. In addition, hepatic gene expression was analyzed to evaluate the similarity with known biological responses. Based on these data, we evaluated the adequacy of PXB mice as an in vivo experimental model to evaluate the key events of the porphyria-mediated cytotoxicity MOA in humans.

Materials and Methods

All animal experiments in this study were approved by the Institutional Animal Care and Use Committee of Sumitomo Chemical Co, Ltd and performed in accordance with *The Guide for Animal Care and Use of Sumitomo Chemical Co, Ltd.* All experiments using PXB mice and samples collected from PXB mice were approved in accordance with *The Guide for Biosafety of Sumitomo Chemical Co, Ltd.*

Animals and Husbandry

Male PXB mice aged 16 to 19 weeks were purchased from PhoenixBio Co, Ltd. Cryopreserved human hepatocytes of BD195 (a healthy 2-year-old Hispanic female; cause of death, motor vehicle accident; nonsmoker; serologically negative for HIV 1 and 2, human T lymphotropic virus 1 and 2, cytomegalovirus, hepatitis B virus, and hepatitis C virus) were used as donor cells for the lot of chimeric mice used in this study. Since the human albumin (hAlb) concentration in chimeric mouse blood correlates well with the replacement index,[13] the hAlb concentration in the blood samples was measured to estimate the replacement index of human hepatocyte in chimeric mouse livers. The replacement indices in chimeric mice used in this study were estimated by the supplier to be in the range of 81% to 97%.

Animals were acclimated to laboratory conditions for 7 days. On the day of initiation of dosing, animals were assigned to each group by a stratified randomization method based upon body weights and replacement index of human hepatocytes estimated by hAlb concentrations, so that there was no significant difference in arithmetic mean of body weights and geometric mean of hAlb concentrations, respectively, among the groups. Animals were housed in a barrier system animal room. During the course of the study, the environmental conditions in

the animal room were targeted within a temperature range of 22 to 26 °C and a relative humidity range of 40% to 70%, with frequent ventilation (more than 10 times per hour) and a 12-hour light (8:00-20:00)/12-hour dark (20:00-8:00) illumination cycle. A commercially available powdered diet for rodents fortified with vitamin C (300 mg/100 g), sterilized by ^{60}Co (30 kGy) irradiation (CRF-1 with vitamin C, Oriental Yeast Co, Ltd), and filtered tap water were provided ad libitum throughout the study.

Study Design

5-Aminolevulinic acid hydrochloride (CAS No: 5451-09-2) was purchased from Tokyo Chemical Industry Co, Ltd. PXB mice (6-9 animals/dose) were fed diets containing 0 (control) or 7000 ppm ALA (preliminary experiment, experiment I), and 0 (control), 3500, or 5000 ppm ALA (main experiment, experiment II), respectively, for 28 days. Dose levels were selected based on a previously reported rat 28-day study.[23] All animals were observed daily throughout the study. Body weights and food consumption were measured approximately once weekly and once or twice weekly, respectively.

In experiment I, administration of 7000 ppm ALA resulted in moribundity, indicated by decreased spontaneous activity, piloerection, and ptosis, in 4 of 7 animals, and 2 animals were found dead on day 21 and 27. Based on the presence of similar adverse clinical observations, the remaining 2 moribund animals were assigned to an early termination necropsy on day 21. These animals found dead or moribund were excluded from the evaluation of this study. Based on the results of experiment I, lower doses (3500 and 5000 ppm) were selected for experiment II. Unlike the 4 animals euthanized or found dead, all 3 surviving animals did not show excessive toxicity, as shown in Table 1 and Figure 1 (in life data, blood biochemistry, and histology) which would prevent meaningful evaluation. Therefore, data from these 3 surviving animals in the 7000 ppm group (experiment I) were represented as well as the animals from experiment II.

Measurement of Liver Concentration of PPIX

Approximately 200 mg of liver samples from all animals were collected at necropsy. Protoporphyrin IX was extracted from the liver sample according to a previously described method[34,35] with modifications. Each liver sample was homogenized in 7 mL methanol:0.1 N NH$_4$OH (9:1 vol/vol, basic methanol), and the homogenate was centrifuged at 10,000g for 10 minutes below 4 °C, and the supernatant was saved in a 15 mL centrifuge tube. The pellet was resuspended in 5 mL basic methanol, sonicated for 30 seconds with a sonicator, and centrifuged at 10,000g for 10 minutes below 4 °C. The supernatant was pooled in the same 15 mL centrifuge tube and stored at −80 °C until purification.

Supernatants were purified using an Oasis MAX μElution Plate (Waters Corporation). First, all supernatant samples were mixed with 10 μL of 1 ppm internal standard (PPIX-d4), which was obtained by diluting with basic methanol, and centrifuged at

20,380g for 15 minutes below 4 °C. Then the purification plate was equilibrated with 400 μL of methanol and water using a vacuum manifold (Aspiration pressure: 5 inHg). Then, 700 μL of the supernatants were loaded into the wells, and the analytes were trapped in the solid phase using the vacuum manifold. After being washed with 400 μL of 5% ammonia solution, 200 μL of methanol, and 200 μL of cyclohexane, PPIX and the internal standard (PPIX-d4) were eluted with 75 μL of methanol containing 2% formic acid. The eluted samples were analyzed by liquid chromatography-mass spectrometry (LC/MS) according to the previously described method[36] with modifications. As with the liver extract samples, calibration samples were also analyzed. These samples were prepared by purifying serially diluted PPIX in the same manner. After the LC/MS analysis, the peak areas of the analytes in the samples were computed and quantified using Xcalibur v2.0.7 (Thermo Fisher Scientific). The calculated value of each sample was normalized to the corresponding weight of the collected liver sample.

Blood Biochemistry

Blood was collected via the abdominal aorta under isoflurane (Isoflurane Inhalation solution, Mylan Inc) anesthesia without prior fasting. The following parameters were determined in the plasma derived from whole blood collected into lithium heparin anticoagulant, clinical biochemistry analyzer JCA-BM6050 (JEOL, Ltd): total protein, Alb, albumin/globulin ratio, glucose, total cholesterol, phospholipids, triglycerides, total bilirubin, AST, ALT, alkaline phosphatase (ALP), lactate dehydrogenase (LDH), and γ-glutamyl transpeptidase (γ-GTP). Also, a part of the plasma sample was used in an enzyme-linked immunosorbent assay system by PhoenixBio Co, Ltd to measure the human-specific ALT1 (hALT1) concentration as previously reported.[14]

Liver Histopathology

At sacrifice, livers were collected, weighed, and transversely cut. Two slices from the left lateral lobe and a segment of duodenum were removed from all animals and fixed in 10% neutral buffered formalin for 24 hours. To demonstrate appropriate administration of bromodeoxyuridine (BrdU), a cross-segment of duodenum was embedded in paraffin along with the liver slices. All paraffin tissues were sectioned, stained with hematoxylin and eosin (H&E), and examined by light microscopy. Histopathological changes in areas of human hepatocytes were evaluated by standard toxicologic pathological criteria, and the pathological lesions in each animal were given one of 4 grades (slight, mild, moderate, or severe). Areas of human cells could be readily distinguished from areas of mouse cells as the human cells had clear cytoplasm with lipid droplets, small nuclei, and were arranged with less orderly arranged cords of cells, whereas mouse cells tended to be eosinophilic without lipid droplets, had larger and more variably sized nuclei, and had more orderly arranged cords of hepatocytes. These differences have been previously validated using immunohistochemical stains for STEM121. Additionally, serial

Table 1. Effects of ALA Treatment on Clinical Signs, Body Weight, Food Consumption, Liver Weight, Blood Biochemical Parameters, and Liver Histopathology.

	Examination II			Examination I	
Dose	Control	3500 ppm	5000 ppm	Control	7000 ppm
Number of animals examined	6	9	8	6	3
Clinical signs[a]					
Red urine	-[b]	Day 5-26 (9)	Day 5-28 (8)	-	Day 2-28 (3)
Colored stool	-	-	-	-	Day 13-27 (2)
Final body weight	-	7%[c]	7%[d]	-	17%[c]
Total food consumption	-	23%[c]	24%[c]	-	34%[c]
Average test substance intake (mg/kg/d)	-	380.6	536.8	-	686.0
Liver weight (absolute)	-	1%[e]	0%	-	22%[e]
Liver weight (relative)	-	7%[f]	8%[f]	-	6%[e]
Blood biochemical parameters[g]					
TP (g/dL)	5.1 ± 0.4	5.5 ± 0.3	5.3 ± 0.3	5.3 ± 0.2	5.2 ± 0.4
Alb (g/dL)	3.6 ± 0.3	3.9 ± 0.2	3.7 ± 0.2	3.7 ± 0.1	3.5 ± 0.3
A/G ratio	2.34 ± 0.06	2.45 ± 0.13	2.29 ± 0.15	2.43 ± 0.12	2.08 ± 0.07[h]
Glu (mg/dL)	167 ± 11	139 ± 20[h]	130 ± 11[h]	156 ± 20	133 ± 22
T-Cho (mg/dL)	62 ± 10	64 ± 7	91 ± 26	82 ± 11	146 ± 54
PL (mg/dL)	93 ± 11	109 ± 17	153 ± 43[i]	124 ± 18	242 ± 94
TG (mg/dL)	54 ± 5	73 ± 19	85 ± 26	77 ± 15	82 ± 30
Histopathological findings (liver, human region)[j]					
Steatosis, hepatocyte	6	9	8	6	3
$\pm$			1		
+	6	9	7	6	2
2+					1
Increased, mitosis, hepatocyte	0	0	4	0	2
$\pm$			4		1
+					1
Necrosis, single cell, diffuse	0	5	6	0	3
$\pm$		4	4		
+		1	2		3
Yellowish, brown pigment[k]	0	0	5	0	3
$\pm$			5		1

(continued)

sections of tissues from 2 control animals and two 5000 ppm animals were stained with H&E, Berlin blue, Schmorl, and Hall stains to evaluate the yellowish-brown pigmentation observed by light microscopic examination.

Hepatocyte Replicative DNA Synthesis Determined as BrdU Labeling Indices

Hepatocyte replicative DNA synthesis was individually determined for the livers from all surviving animals.

Bromodeoxyuridine (Sigma-Aldrich Corp) was dissolved in dimethyl sulfoxide to a concentration of 40 mg/mL. Alzet osmotic pumps (Model 2001, Alzet Corporation) were filled with 200 μL of this solution, and then incubated in saline at 37 to 42 °C for about 3 to 5 hours before implantation. On the day prior to 7 days before the scheduled euthanasia, the filled pumps were implanted subcutaneously in the back region of animals under isoflurane anesthesia and remained there until necropsy, with a release rate of 40 μg/h (total release of 6720 μg).
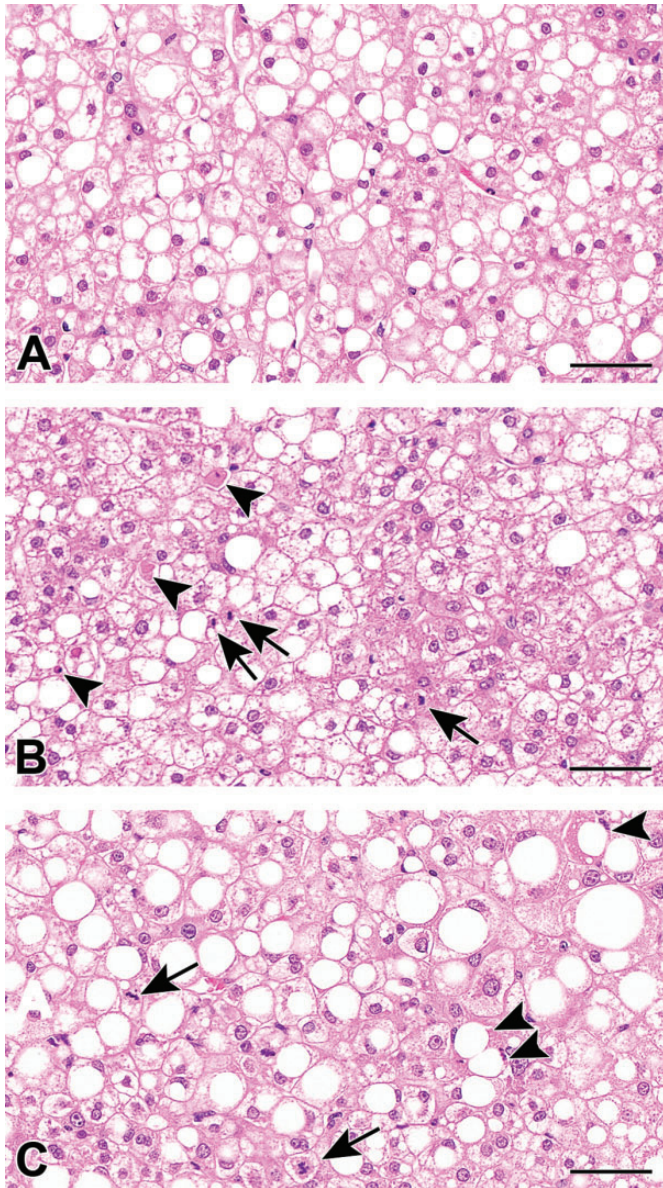
Figure 1. Photographs of histopathological findings of the control (A), ALA 5000 ppm treated (B), and 7000 ppm treated (C) groups. Hepatocellular necrosis (black arrow heads) and mitosis (black arrows) in ALA treated groups. Hematoxylin and eosin. Scale bar = 50 µm. ALA indicates 5-aminolevulinic acid.

Tissue sections were stained immunohistochemically using BrdU monoclonal antibody (Agilent Technologies; Code No. M0744, 250 times diluted), biotinylated rabbit-antimouse F(ab′)2 (Agilent Technologies; Code No. E0413, diluted 400 times), VECTASTAIN Elite ABC Standard Kit (Vector Laboratories, Inc; Code No. PK-6100), and diaminobenzidine (DAB) development to determine BrdU labeling indices. We used an image analysis system to evaluate the BrdU labeling indices of human hepatocytes in the chimeric mice, as these systems can evaluate more hepatocytes than when evaluated manually. Glass slides were scanned at 20× magnification using the Olympus VS120 virtual slide scanning system (Olympus), and Definiens Tissue Studio software (Definiens) was used to generate image analysis solutions. We manually selected areas of human hepatocytes that could be clearly distinguished from mouse hepatocytes and did not include a boundary region between mouse and human areas. Slides were evaluated in a blinded manner, and custom-made image analysis algorithms were applied to the digital slides to automatically detect and quantify the number of DAB positive and negative hepatocytes. The total number of evaluated cells was more than 10,000 per animal. Sections of duodenum embedded with liver slices were also prepared and stained immunohistochemically on the same glass slide as the liver sections using BrdU monoclonal antibody to serve as a positive control to confirm appropriate administration of BrdU but were not counted.

Gene Expression Analysis

After necropsy, a piece of liver from each animal was removed and stored in RNA stabilization solution (Ambion) at room temperature for 24 hours. After that, these samples were moved to a deep freezer at $-80\,°C$ until analyzed for gene expression. Remaining liver tissue after sampling was frozen in liquid nitrogen and stored at $-80\,°C$.

Messenger RNA measurement of genes of enzymes in the porphyrin biosynthesis/catabolism pathway and porphyrin transporters in the liver was performed by Sumika Technoservice Corporation. Total RNA was extracted from livers using the RNeasy Mini kit (Qiagen) in accordance with manufacturer instructions. Complementary DNA was prepared from total RNA by reverse transcription using the High Capacity cDNA Reverse Transcription Kit (Applied Biosystems) according to the manufacturer instructions. In all animals, expression levels of each gene and human β-actin (used as reference gene and for normalization) were determined by quantitative real-time polymerase chain reaction (PCR) assay following the instruction manual of the PCR system (Applied Biosystems 7500 Fast Real-Time PCR System, Applied Biosystems). The primer and probe sets are shown in Supplemental Table 1.

The reaction mixture (25 µL) contained 2× TaqMan Universal Master Mix (Applied Biosystems; 12.5 µL), each primer (forward and reverse, 0.9 µM each), probe (0.25 µM), and cDNA (2 µL of 1/4 diluted solution). After incubation at 50 °C for 2 minutes and 95 °C for 10 minutes, the PCR reaction was performed for 40 cycles: denaturation at 95 °C for 15 seconds, annealing and extension at 60 °C for 1 minute.

Statistical Analyses

Body weights were evaluated as those including osmotic minipump after implantation. The following comparison procedures were used for analysis of data for body weight, body weight gains, food consumption, blood biochemistry, absolute and relative liver weights, PPIX concentration, cell proliferation rate, and gene expression level.

For experiment I, the *F* test was applied to compare the treated group with the control group. If the variance was homogeneous, the Student *t* test was used. If the variance was heterogeneous, the Aspin-Welch test was used.

For experiment II, Bartlett test was employed to compare variances among the groups. If the variance was homogeneous, Dunnett test was applied to compare the groups given the test substance with the control. If the variance was heterogeneous, Steel test was used.

For mRNA expression, the data are expressed as the fold-change value relative to the control group of each experiment.

Results

General Observations

Clinical signs, body weights, body weight gains, and food consumption are presented in Table 1. Some animals in all
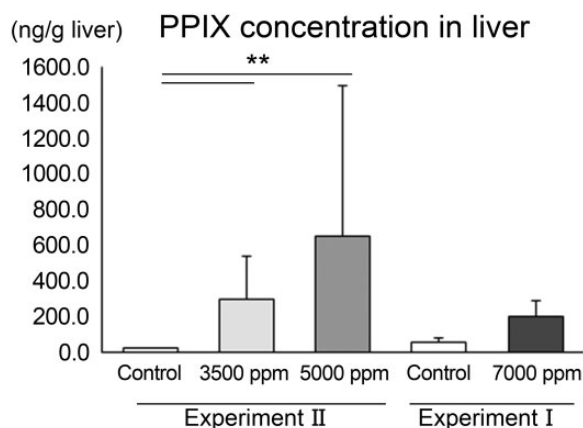
Figure 2. Effect of ALA treatment on PPIX concentration in the liver analyzed by LC/MS. Significantly different from the control at **$P <.01$. N = 6, 9, 9, and 3 for the respective groups. ALA indicates 5-aminolevulinic acid; LC/MS, liquid chromatography-mass spectrometry; PPIX, protoporphyrin IX.

treatment groups showed red urine and/or colored stool, suggesting increased biliary or urinary excretion of porphyrins and/or their metabolites. Statistical significance or trend toward decrease in body weights, body weight gains, and food consumption in mice administered ALA compared to the control groups was observed. As mentioned in the Materials and Methods section, animals found dead or moribund were excluded from the evaluation of experiment I, and the data from the 3 surviving animals subjected to the scheduled necropsy without excessive toxicity are shown in Table 1 and were used for interpretation of this study.

Accumulation of PPIX in the Liver

As shown in Figure 2, LC/MS analysis revealed increases of PPIX level in the liver of all treatment groups, with statistical significance at 3500 and 5000 ppm and a tendency at 7000 ppm, although there were no clear dose-responses across treatment groups.

Blood Biochemistry

As shown in Table 2, increases in ALT, AST, ALP, LDH, and/or γ-GTP were observed in all treatment groups, with most reaching statistical significance. In addition, a statistically significant or trend toward increase in hALT1 concentration was observed in all treatment groups, indicating that human hepatocytes likely were damaged by the administration of ALA.

Histopathological Examination

In PXB mice, humanized liver consists of transplanted human hepatocytes and host mouse-derived hepatocytes, and both areas were easily distinguishable by H&E staining[19] because human hepatocytes showed clear cytoplasm and contained lipid droplets, while mouse hepatocytes showed eosinophilic cytoplasm.[37] Based on these histological

Table 2. Effect of ALA Treatment on Blood Biochemical Parameters in Serum Represented as Mean ± SD.

	Experiment II			Experiment I	
Dose Number of animals examined	Control 5[a]	3500 ppm 8-9[a]	5000 ppm 7-8[a]	Control 6	7000 ppm 3
T-Bil (mg/dL)	0.12 ± 0.03	0.12 ± 0.03	0.13 ± 0.04	0.07 ± 0.01	0.16 ± 0.06
AST (U/L)	203 ± 36	344 ± 146	507 ± 149[b]	324 ± 169	1143 ± 282
ALT (U/L)	216 ± 35	352 ± 123	597 ± 271[c]	356 ± 151	1366 ± 521[c]
ALP (U/L)	318 ± 33	322 ± 46	368 ± 47	275 ± 18	536 ± 26[c]
LDH (U/L)	706 ± 174	814 ± 232	1140 ± 248[c]	858 ± 257	2241 ± 1068
γ-GTP (U/L)	17 ± 5	18 ± 7	33 ± 15	14 ± 5	78 ± 66
hALT1 (ng/mL)	64 ± 10	87 ± 32	147 ± 73 (P = .07)	65 ± 26	521 ± 476

Abbreviations: ALA, 5-aminolevulinic acid; ALP, alkaline phosphatase; ALT, alanine aminotransferase; AST, aspartate aminotransferase; hALT1, human-specific ALT1; LDH, lactate dehydrogenase; SD, standard deviation; T-Bil, total bilirubin; γ-GTP, γ-glutamyl transpeptidase.

[a]Parameters were not determined for 1 animal in each group because of insufficient sample volume.

[b]Significantly changed from control values ($P < .05$).

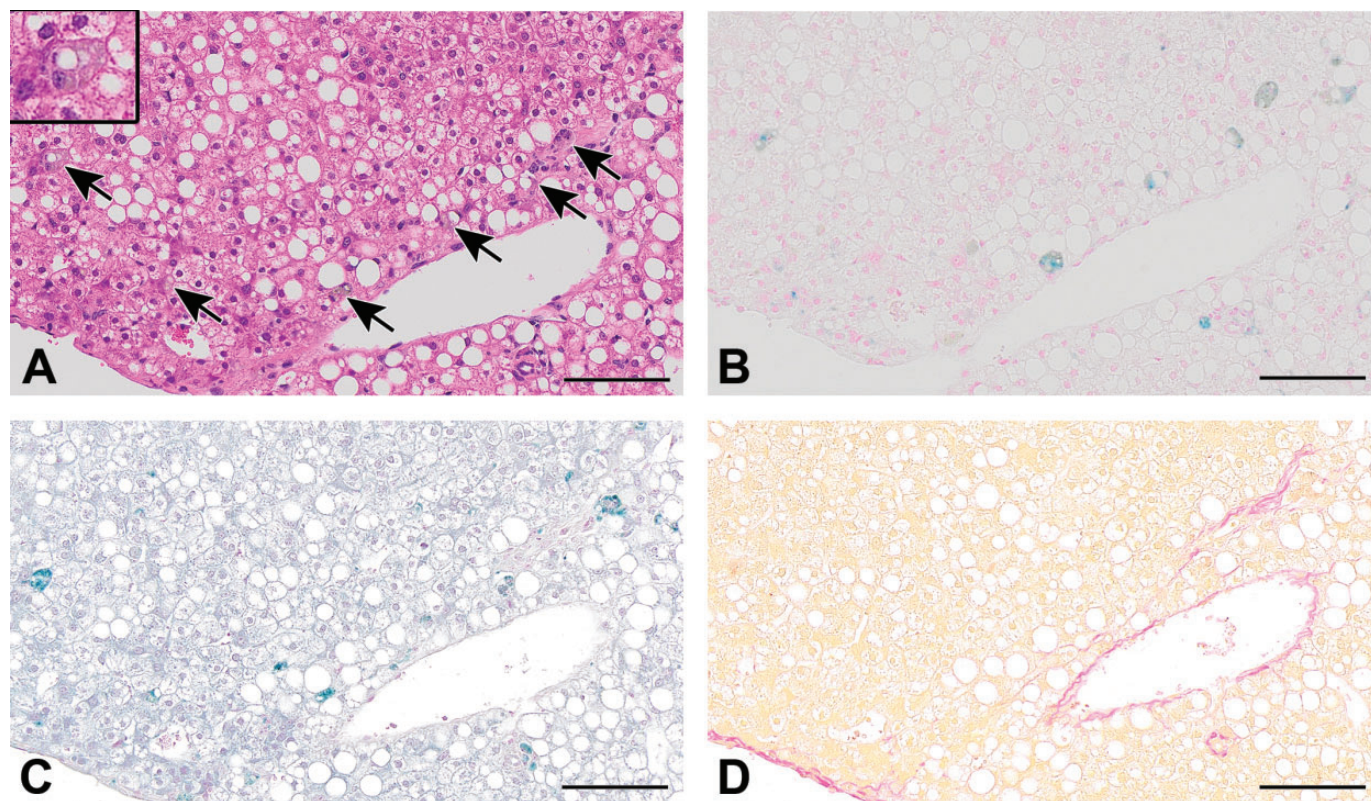[c]Significantly changed from control values ($P < .01$).

Figure 3. Serial sections of 5000 ppm treated liver stained with hematoxylin and eosin stain (A), Berlin blue stain for detecting iron (B), Schmorl stain for detecting lipofuscin (C), and Hall stain for detecting bilirubin (D). Yellowish-brown pigment in hepatocytes and macrophages including Kupffer cells (indicated by black arrows and in enlarged inset image in A) is stained blue by Berlin blue stain or blue-green by Schmorl stain, but negative by Hall stain. Scale bar = 100 μm.

differences, histopathological findings in human hepatocellular areas were evaluated. Results of histopathological examination of the liver are shown in Table 1 and Figure 1. Hepatocellular injury was observed in all treatment groups, including single cell necrosis and associated increased mitoses and/or yellowish-brown pigmentation in hepatocytes and macrophages, including Kupffer cells. The incidences and severities of these histopathological changes tended to increase dose dependently and also were associated with increased liver enzymes including hALT1. In addition, the 4 animals euthanized or found dead showed similar histopathological findings (data not shown), suggesting that the poor general condition in these animals did not affect histopathological evaluation of porphyria-mediated hepatotoxicity and thus ensured the validity of the findings in the 3 surviving animals at 7000 ppm.

Additionally, serial sections of livers from the 2 controls and two 5000 ppm animals were stained with H&E, Berlin blue, Schmorl, and Hall stains, as shown in Figure 3. In animals at 5000 ppm, the yellowish-brown pigment observed in hepatocytes or macrophages, including Kupffer cells, stained positively with Berlin blue and/or Schmorl stains, but negatively with Hall stain, indicating that the yellowish-brown pigment was hemosiderin and lipofuscin but not bilirubin.

Gene Expression Analysis of Enzymes in Porphyrin Biosynthesis Pathway and Porphyrin Transporters

Figure 4 presents the results of the gene expression analysis. Gene expression of ATP-binding cassette (ABC) transporters, ATP-binding cassette subfamily B member 6 (ABCB6) and ATP-binding cassette subfamily G member 2 (ABCG2), changed in relation to ALA treatment, but no significant changes were observed in the expression of enzymes in the porphyrin biosynthesis pathway in human hepatocytes. Gene expression of heme oxygenase 1 (HMOX1) was also changed dose dependently. In addition, a slight increase in uroporphyrinogen III synthase (UROS) expression was observed.

Replicative DNA synthesis

Bromodeoxyuridine labeling index was evaluated in areas of human hepatocytes selected manually based on morphological characteristics as with the histopathological examination. As shown in Figures 5 and 6, statistically significant increases in the index were observed at 3500 and 5000 ppm groups. Although without statistical significance, the labeling index was increased 2-fold at 7000 ppm, and 2 of 3 animals had a labeling index greater than any of the controls. At these dose
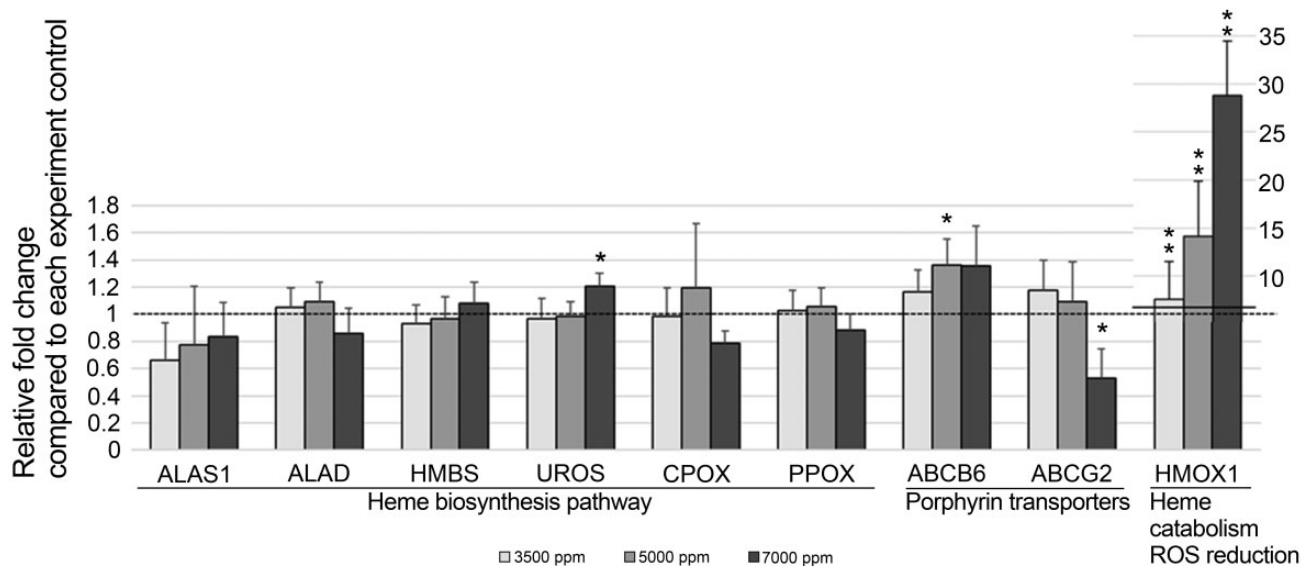
Figure 4. Effect of ALA treatment on gene expression measured by RT-PCR. Expressed as relative fold change compared to the control mean levels. Significantly different from the control at *P < .05 and **P < .01, respectively. N = 6, 9, 9, and 3 for the respective groups. ABCB6 indicates ATP-binding cassette subfamily B member 6, ABCG2, ATP-binding cassette subfamily G member 2; ALA, 5-aminolevulinic acid; ALAS1, 5′-aminolevulinate synthase 1; ALAD, aminolevulinate dehydratase; CPOX, coproporphyrinogen oxidase; HMBS, hydroxymethylbilane synthase; HMOX1, heme oxygenase 1; PPOX, protoporphyrinogen oxidase; ROS, reactive oxygen species; RT-PCR, reverse transcriptase polymerase chain reaction; UROS, uroporphyrinogen III synthase.

levels, single cell necrosis and/or increased mitoses were observed in the histopathological examination.

Discussion

In the present study, we provide novel information on the utility of chimeric mice with humanized liver (PXB mice) to evaluate the key events of the porphyria-mediated cytotoxicity MOA in humans, which could be required to assess human relevance of findings in animals for human risk assessment.

The porphyrinogenic compounds are known to induce liver tumors in rodents via a porphyria-mediated cytotoxicity MOA with key events preceding tumor development that include accumulation of porphyrins, followed by hepatocellular injury, and subsequent regenerative cell proliferation.[5-8] The present study is the first to demonstrate that the administration of ALA, a representative porphyrinogenic compound, induces accumulation of PPIX in an experimental in vivo model of human hepatocytes (Figure 2), which is consistent with reports in ALA-administered rats[23,24,38] and mice[39,40] and in patients with hereditary porphyria.[41]

With regard to the key events following PPIX accumulation, the present study clearly demonstrated that the administration of ALA induced hepatocellular cytotoxicity in human hepatocytes transplanted in PXB mice, which was confirmed by histopathological findings (single cell necrosis in human hepatocellular areas) and blood biochemical alterations, including hALT1 (Table 2). These results indicate that PXB mice can be useful tools for the evaluation of porphyrogenic in

vivo human hepatotoxicity, which complements other studies of hepatotoxicants.[14-18] Also, yellowish-brown pigment was observed in association with the hepatocellular injury which stained with Berlin blue and Schmorl stains (Table 1 and Figure 3), indicating the presence of iron and lipofuscin deposition, respectively. Iron accumulation is considered secondary to porphyria-related perturbation of heme biosynthesis based on evidence that porphyrogenic compounds induce iron deposition in the liver.[6,7] Lipofuscin is an intracellular aggregate of highly oxidized proteins, lipids, and metals,[42] and its accumulation is accelerated under oxidative stress,[43] which is a known mechanism of PPIX-mediated cellular injury.[1] Upregulated gene expression of HMOX1 (Figure 4) is considered to support ALA-induced oxidative stress since it is known to be an adaptive mechanism to protect cells from oxidative damage.[44] In general, hepatocyte injury and pigmentation are characteristically observed in histopathological examination of livers from patients with hereditary porphyria[45] or experimental rodent models of chemically induced porphyria.[46-48] Additionally, it is reported that iron and lipofuscin deposition and HMOX1 gene elevation are observed in human liver from patients with porphyria.[49] Taken together, administration of ALA to PXB mice clearly induced porphyria-mediated hepatocellular cytotoxicity and associated changes which mimic the pathologic nature of the liver in patients with porphyria and animal models of chemically induced porphyria.

Based on these findings, we further examined regenerative proliferation following the cytotoxicity. A sensitive measure of cell proliferation is to assess the rate of S-phase activity of the
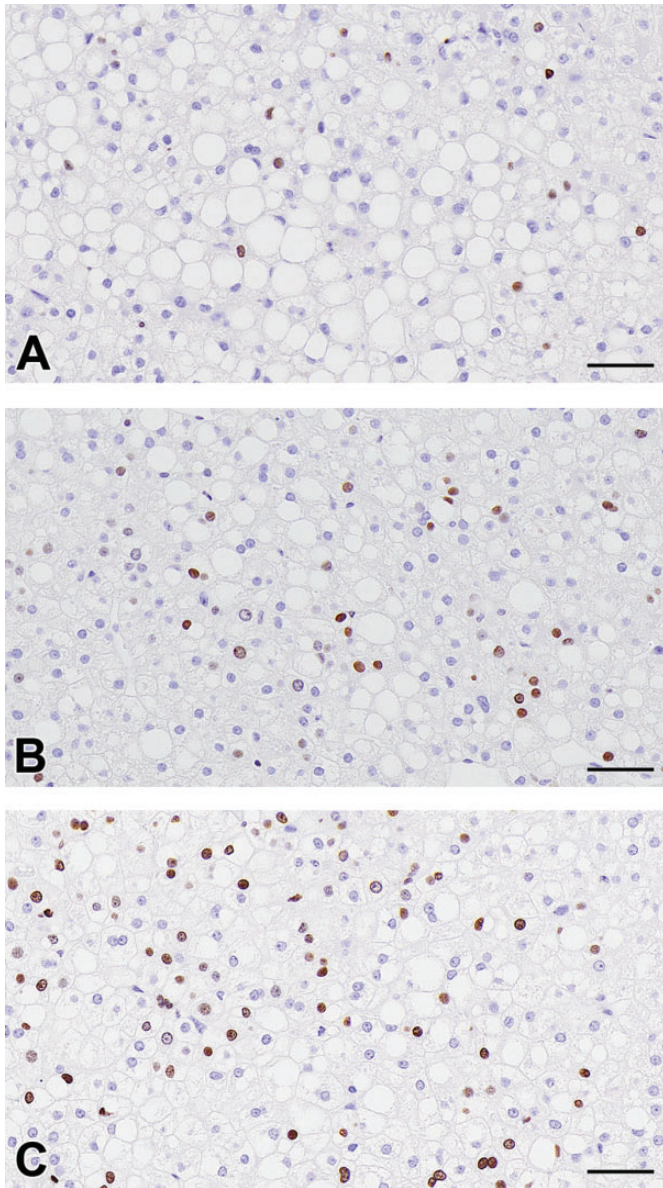
Figure 5. Photographs of immunohistochemical stains for BrdU of the control (A), ALA 5000 ppm treated (B), and 7000 ppm treated (C) groups. Brown nuclei are positively stained for BrdU. Increased BrdU positive hepatocytes in ALA-treated groups. Scale bar = 50 um. ALA indicates 5-aminolevulinic acid, BrdU, bromodeoxyuridine.
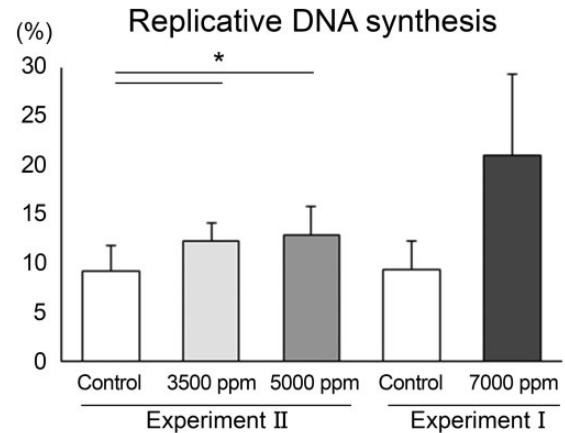

Figure 6. Replicative DNA synthesis was determined as BrdU labeling index of human hepatocytes in the chimeric mouse. N = 6, 9, 9, and 3 for the respective groups. Significantly different from the control at *P <.05. BrdU indicates bromodeoxyuridine.

cell cycle using BrdU incorporation as a marker of DNA synthesis.[50] Thus, the BrdU labeling indices in the human hepatocellular regions were examined in the present study (Figure 6), indicating increases in replicative DNA synthesis in all treatment groups, which were accompanied by increased mitoses observed in the histopathological examination, especially at higher doses. Also, increases in replicative DNA synthesis were noted at all doses and were associated with single cell necrosis observed by histopathological examination. These findings are collectively considered to indicate regenerative proliferation following the cytotoxicity. This proliferative

finding is also observed in livers from patients with hereditary porphyria such as nodular regenerative hyperplasia, indicating that this chimeric mouse model mimics pathologic findings in the livers of patients with porphyria. Several studies demonstrated that transplanted human hepatocytes in PXB mice are responsive to the treatment with human growth hormone[51,52] or epidermal growth factor,[19,21] which are direct hepatocyte mitogens. Our results provide novel evidence that human hepatocytes transplanted in PXB mice are also sensitive to a regenerative proliferative response following cytotoxicity.

As discussed above, the key events of the porphyria-mediated cytotoxicity MOA were clearly detected in the human hepatocytes of PXB mice following administration of ALA, which adequately mimics several features of hereditary porphyria in humans and chemically induced porphyria in experimental rodents. Furthermore, we have evaluated biological alterations of specific enzymes and transporters which are known to be involved in porphyria (Figure 7). As shown in Figure 4, there were significant differences in gene expression of the porphyrin transporters, ABCB6 and ABCG2, both of which are ABC transporters and regulate intracellular porphyrin homeostasis. ABCB6 is oriented to facilitate porphyrin import into mitochondria from the cytoplasm,[53-55] and its expression is known to be upregulated by elevation of cellular porphyrin concentrations in order to mitigate liver damage.[54,56] Therefore, upregulation of ABCB6 occurred as a protective response to PPIX accumulation in PXB mouse liver, as is the case with normal human liver. ABCG2 (also called BCRP [breast cancer resistance protein]) is responsible for the transport of PPIX into the extracellular space.[55,57] Interestingly, it has been reported that ABCG2 deficiency protects against porphyria-induced hepatotoxicity by modulating PPIX distribution, metabolism, and excretion.[57] In the present study, downregulation of ABCG2 was noted in 3 animals in the 7000 ppm group (the other animals died during the study and
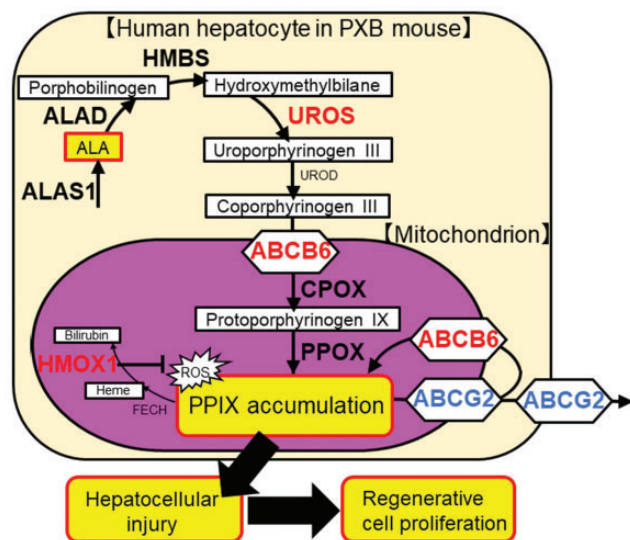
Figure 7. Schematic representation of genes altered by excessive ALA treatment. The genes measured by RT-PCR are indicated by bold letters, with increased expression by red letters, and with decreased expression by blue letters. ABCB6 indicates ATP-binding cassette subfamily B member 6; ABCG2, ATP-binding cassette subfamily G member 2; ALA, 5-aminolevulinic acid; ALAS1, 5′-aminolevulinate synthase 1; ALAD, aminolevulinate dehydratase; CPOX, coporphyrinogen oxidase; FECH, ferrochelatase; HMBS, hydroxymethylbilane synthase; HMOX1, heme oxygenase 1; PPIX, protoporphyrin IX; PPOX, protoporphyrinogen oxidase; ROS, reactive oxygen species; RT-PCR, reverse transcriptase polymerase chain reaction; UROD, uroporphyrinogen decarboxylase; UROS, uroporphyrinogen III synthase.

were eliminated from the evaluation to avoid a non-specific interpretation), which might also be indicative of a protective response to PPIX accumulation in human liver. Taken together, it is suggested that PXB mice represent the normal biological response to PPIX accumulation in human liver caused by porphyrinogenic compounds (Figure 7). Gene expression of porphyrin synthesis enzymes, including rate-limiting enzyme ALAS1, were unaffected by the treatment with ALA except for a slight increase in UROS expression, although ALAS1 is known to be increased in several clinical and experimental porphyrias when heme synthesis is blocked or heme turnover is increased.[58,59] This result suggests the possibility that enhanced porphyrin synthesis did not contribute to ALA-induced PPIX accumulation due to the difference in the pathogenesis of PPIX accumulation (Figure 7).

Overall, we conclude that the PXB mouse is a useful humanized in vivo animal model to evaluate the key events of the porphyria-mediated cytotoxicity MOA in humans. Therefore, robust and reliable MOA data for porphyria-induced hepatocellular tumors could be obtained by using the PXB mouse, which could be used to enable interpretation of interspecies differences between mice and humans and to evaluate human relevancy of this MOA more accurately if it occurs in mice associated with chemical administration.

ORCID iDs

Ayumi Eguchi https://orcid.org/0000-0002-1961-2803
Samuel M. Cohen https://orcid.org/0000-0002-5047-0962

Supplemental Material

Supplemental material for this article is available online.

References

1. Afonso S, Vanore G, Batlle A. Protoporphyrin IX and oxidative stress. *Free Radic Res*. 2009;31(3):161-170.
2. Maitra D, Carter EL, Richardson R, et al. Oxygen and conformation dependent protein oxidation and aggregation by porphyrins in hepatocytes and light-exposed cells. *Cell Mol Gastroenterol Hepatol*. 2019;8(4): 659-682. e651.
3. Maitra D, Elenbaas JS, Whitesall SE, Basrur V, D'Alecy LG, Omary MB. Ambient light promotes selective subcellular proteotoxicity after endogenous and exogenous porphyrinogenic stress. *J Biological Chem*. 2015; 290(39):23711-23724.
4. Singla A, Griggs NW, Kwan R, et al. Lamin aggregation is an early sensor of porphyria-induced liver injury. *J Cell Sci*. 2013;126(Pt 14):3105-3112.
5. Cohen SM. Evaluation of possible carcinogenic risk to humans based on liver tumors in rodent assays. *Toxicol Pathol*. 2010;38(3):487-501.
6. Holsapple MP, Pitot HC, Cohen SM, et al. Mode of action in relevance of rodent liver tumors to human cancer risk. *Toxicol Sci*. 2006;89(1):51-56.
7. Smith AG, Foster JR. The association between chemical-induced porphyria and hepatic cancer. *Toxicol Res*. 2018;7(4):647-663.
8. Felter SP, Foreman JE, Boobis A, et al. Human relevance of rodent liver tumors: Key insights from a Toxicology Forum workshop on nongenotoxic modes of action. *Regul Toxicol Pharmacol*. 2018;92:1-7.
9. Sardh E, Wahlin S, Bjornstedt M, Harper P, Andersson DE. High risk of primary liver cancer in a cohort of 179 patients with acute hepatic porphyria. *J Inherit Metab Dis*. 2013;36(6):1063-1071.
10. Boobis AR, Cohen SM, Dellarco V, et al. IPCS framework for analyzing the relevance of a cancer mode of action for humans. *Crit Rev Toxicol*. 2006;36(10):781-792.
11. Meuleman P, Libbrecht L, De Vos R, et al. Morphological and biochemical characterization of a human liver in a uPA-SCID mouse chimera. *Hepatol*. 2005;41(4):847-856.

12. Tateno C, Miya F, Wake K, et al. Morphological and microarray analyses of human hepatocytes from xenogeneic host livers. *Lab Invest*. 2013;93(1): 54-71.

13. Tateno C, Yoshizane Y, Saito N, et al. Near completely humanized liver in mice shows human-type metabolic responses to drugs. *Am J Pathol*. 2004; 165(3):901-912.

14. Ishida Y, Yamasaki C, Iwanari H, et al. Detection of acute toxicity of aflatoxin B1 to human hepatocytes in vitro and in vivo using chimeric mice with humanized livers. *PLoS One*. 2020;15(9):e0239540.

15. Kakuni M, Morita M, Matsuo K, et al. Chimeric mice with a humanized liver as an animal model of troglitazone-induced liver injury. *Toxicol Lett*. 2012;214(1):9-18.

16. Sato Y, Yamada H, Iwasaki K, et al. Human hepatocytes can repopulate mouse liver: histopathology of the liver in human hepatocyte-transplanted chimeric mice and toxicologic responses to acetaminophen. *Toxicol Pathol*. 2008;36(4):581-591.

17. Foster JR, Jacobsen M, Kenna G, et al. Differential effect of troglitazone on the human bile acid transporters, MRP2 and BSEP, in the PXB hepatic chimeric mouse. *Toxicol Pathol*. 2012;40(8):1106-1116.

18. Nihira K, Nan-Ya KI, Kakuni M, et al. Chimeric mice with humanized livers demonstrate human-specific hepatotoxicity caused by a therapeutic antibody against TRAIL-receptor 2/death receptor 5. *Toxicol Sci*. 2019; 167(1):190-201.

19. Okuda Y, Kushida M, Kikumoto H, et al. Evaluation of the human relevance of the constitutive androstane receptor-mediated mode of action for rat hepatocellular tumor formation by the synthetic pyrethroid momfluorothrin. *J Toxicol Sci*. 2017;42(6):773-788.

20. Yamada T. Case examples of an evaluation of the human relevance of the pyrethroids/pyrethrins-induced liver tumours in rodents based on the mode of action. *Toxicol Res (Camb)*. 2018;7(4):681-696.

21. Yamada T, Okuda Y, Kushida M, et al. Human hepatocytes support the hypertrophic but not the hyperplastic response to the murine non-genotoxic hepatocarcinogen sodium phenobarbital in an in vivo study using a chimeric mouse with humanized liver. *Toxicol Sci*. 2014; 142(1):137-157.

22. Hunter GA, Ferreira GC. Molecular enzymology of 5-Aminolevulinate synthase, the gatekeeper of heme biosynthesis. Biochimica et Biophysica Acta (BBA). *Prot Proteom*. 2011;1814(11):1467-1473.

23. Miyanari S. Single and 28-day oral dose toxicity study of 5-aminolevulinic acid phosphate in rats. *Jpn Pharmacol Ther*. 2011;39(5):503-511.

24. Miyanari S. 13-week oral dose toxicity study of 5-aminolevulinic acid phosphate in rats. *Jpn Pharmacol Ther*. 2011;39(5):513-524.

25. PMDA. Alaglio Divided Granules 1.5 g (aminolevulinic acid hydrochloride), Product information. Published 2017. Accessed December 23, 2020. https://www.pmda.go.jp/drugs/2017/P20171006001/171155000_22900AMX00989000_B100_1.pdf

26. FDA. Gleolan (aminolevulinic acid hydrochloride), Approval Letter(s); Published 2017. Updated June 6, 2020. Accessed December 23, 2020. https://www.accessdata.fda.gov/drugsatfda_docs/nda/2017/208630Orig1s000Approv.pdf

27. EMA. Gliolan, Product information. Published 2020. Accessed December 23, 2020. https://www.ema.europa.eu/en/documents/product-information/gliolan-epar-product-information_en.pdf

28. Chung IW, Eljamel S. Risk factors for developing oral 5-aminolevulinic acid-induced side effects in patients undergoing fluorescence guided resection. *Photodiagnosis Photodyn Ther*. 2013;10(4):362-367.

29. Honorato-Cia C, Martinez-Simon A, Cacho-Asenjo E, Guillen-Grima F, Tejada-Solis S, Diez-Valle R.Safety profile of 5-aminolevulinic acid as a surgical adjunct in clinical practice: a review of 207 cases from 2008 to 2013. *J Neurosurg Anesthesiol*. 2015;27(4):304-309.

30. Kim JH, Yoon HK, Lee HC, et al. Preoperative 5-aminolevulinic acid administration for brain tumor surgery is associated with an increase in postoperative liver enzymes: a retrospective cohort study. *Acta Neurochir (Wien)*. 2019;161(11):2289-2298.

31. Marbacher S, Klinger E, Schwyzer L, et al. Use of fluorescence to guide resection or biopsy of primary brain tumors and brain metastases. *Neurosurg Focus*. 2014;36(2):E10.

32. Offersen CM, Skjoeth-Rasmussen J. Evaluation of the risk of liver damage from the use of 5-aminolevulinic acid for intra-operative identification and resection in patients with malignant gliomas. *Acta Neurochir (Wien)*. 2017;159(1):145-150.

33. Teixidor P, Arraez MA, Villalba G, et al. Safety and efficacy of 5-aminolevulinic acid for high grade glioma in usual clinical practice: a prospective cohort study. *PLoS One*. 2016;11(2):e0149244.

34. Kawamura S, Kato T, Matsuo M, Katsuda Y, Yasuda M. Species difference in protoporphyrin IX accumulation produced by an N-phenylimide herbicide in embryos between rats and rabbits. *Toxicol Appl Pharmacol*. 1996;141(2):520-525.

35. Matsumoto H, Duke SO. Acifluorfen-methyl effects on porphyrin synthesis in Lemna pausicostata Hegelm. 6746. *J Agri Food Chem*. 1990; 38(11):2066-2071.

36. Moulin M, McCormac AC, Terry MJ, Smith AG. Tetrapyrrole profiling in Arabidopsis seedlings reveals that retrograde plastid nuclear signaling is not due to Mg-protoporphyrin IX accumulation. *Proc Natl Acad Sci U S A*. 2008;105(39):15178-15183.

37. Tateno C, Kojima Y. Characterization and applications of chimeric mice with humanized livers for preclinical drug development. *Labora Animal Res*. 2020;36:2.

38. Van Hillegersberg R, Van den Berg JW, Kort WJ, Terpstra OT, Wilson JH. Selective accumulation of endogenously produced porphyrins in a liver metastasis model in rats. *Gastroenterol*. 1992;103(2):647-651.

39. Anderson KE, Drummond GS, Freddara U, Sardana MK, Sassa S. Porphyrogenic effects and induction of heme oxygenase in vivo by delta-aminolevulinic acid. *Biochim Biophys Acta*. 1981;676(3): 289-299.

40. Peng Q, Moan J, Warloe T, Nesland JM, Rimington C. Distribution and photosensitizing efficiency of porphyrins induced by application of exogenous 5-aminolevulinic acid in mice bearing mammary carcinoma. *Int J Cancer*. 1992;52(3):433-443.

41. Bloomer JR. Hepatic protoporphyrin metabolism in patients with advanced protoporphyric liver disease. *Yale J Biol Med*. 1997;70(4): 323-330.

42. Cindrova-Davies T, Fogarty NME, Jones CJP, Kingdom J, Burton GJ. Evidence of oxidative stress-induced senescence in mature, post-mature and pathological human placentas. *Placenta*. 2018;68:15-22.

43. Kakimoto Y, Okada C, Kawabe N, et al. Myocardial lipofuscin accumulation in ageing and sudden cardiac death. *Sci Rep*. 2019;9(1):3304.

44. Poss KD, Tonegawa S. Reduced stress defense in heme oxygenase 1-deficient cells. *Proc Natl Acad Sci U S A*. 1997;94(20):10925-10930.

45. Lee KG, Hyun JJ, Seo YS, et al. Liver cirrhosis induced by porphyria cutanea Tarda: a case report and review. *Gut Liver*. 2010;4(4): 551-555.

46. Choi SW, Han JH, Lim KT, et al. Effect of ursodeoxycholic acid on experimental hepatic porphyria induced by griseofulvin. *J Korean Med Sci*. 1991;6(2):146-156.

47. Nicolas JM, Chanteux H, Mancel V, et al. N-alkylprotoporphyrin formation and hepatic porphyria in dogs after administration of a new antiepileptic drug candidate: mechanism and species specificity. *Toxicol Sci*. 2014;141(2):353-364.

48. Stejskal R, Itabashi M, Stanek J, Hruban Z. Experimental porphyria induced by 3-(2,4,6-trimethylphenyl)-thioethyl)-4 methylsydnone. *Virchows Arch B Cell Pathol*. 1975;18(2):83-100.

49. Yasuda M, Erwin AL, Liu LU, et al. Liver transplantation for acute intermittent porphyria: Biochemical and pathologic studies of the explanted liver. *Mol Med*. 2015;21(1):487-495.

50. Wood CE, Hukkanen RR, Sura R, et al. Scientific and Regulatory Policy Committee (SRPC) review: Interpretation and use of cell proliferation data in cancer risk assessment. *Toxicol Pathol*. 2015;43(6): 760-775.

51. Masumoto N, Tateno C, Tachibana A, et al. GH enhances proliferation of human hepatocytes grafted into immunodeficient mice with damaged liver. *J Endocrinol*. 2007;194(3):529-537.

52. Tateno C, Kataoka M, Utoh R, et al. Growth hormone-dependent pathogenesis of human hepatic steatosis in a novel mouse model bearing a

human hepatocyte-repopulated liver. *Endocrinol*. 2011;152(4): 1479-1491.

53. Krishnamurthy P, Schuetz JD. The role of ABCG2 and ABCB6 in porphyrin metabolism and cell survival. *Curr Pharm Biotechnol*. 2011;12(4): 647-655.

54. Krishnamurthy PC, Du G, Fukuda Y, et al. Identification of a mammalian mitochondrial porphyrin transporter. *Nature*. 2006;443(7111): 586-589.

55. Sachar M, Anderson KE, Ma X. Protoporphyrin IX: the good, the bad, and the ugly. *J Pharmacol Exp Ther*. 2015;356(2):267-275.

56. Krieg RC, Messmann H, Schlottmann K, et al. Intracellular localization is a cofactor for the phototoxicity of protoporphyrin IX in the gastrointestinal tract: in vitro study. *Photochem Photobiol*. 2003; 78(4):393-399.

57. Hagiwara S, Nishida N, Park AM, Sakurai T, Kawada A, Kudo M. Impaired expression of ATP-binding cassette transporter G2 and liver damage in erythropoietic protoporphyria. *Hepatol*. 2015;62(5): 1638-1639.

58. Tschudy DP, Perlroth MG, Marver HS, Collins A, Hunter G Jr, Rechcigl M Jr. Acute intermittent porphyria: the first "Overproduction Disease" localized to a specific enzyme. *Proc Natl Acad Sci U S A*. 1965;53(4):841-847.

59. Bloomer JR, Reuter RJ, Morton KO, Wehner JM. Enzymatic formation of zinc-protoporphyrin by rat liver and its potential effect on hepatic heme metabolism. *Gastroenterol*. 1983;85(3):663-668.